Touch Your Robots Without Tactile Sensors

Wanjia Fu[1*], Hongyu Li[1*], Ivy X. He[1], Stefanie Tellex[1], and Srinath Sridhar[1]

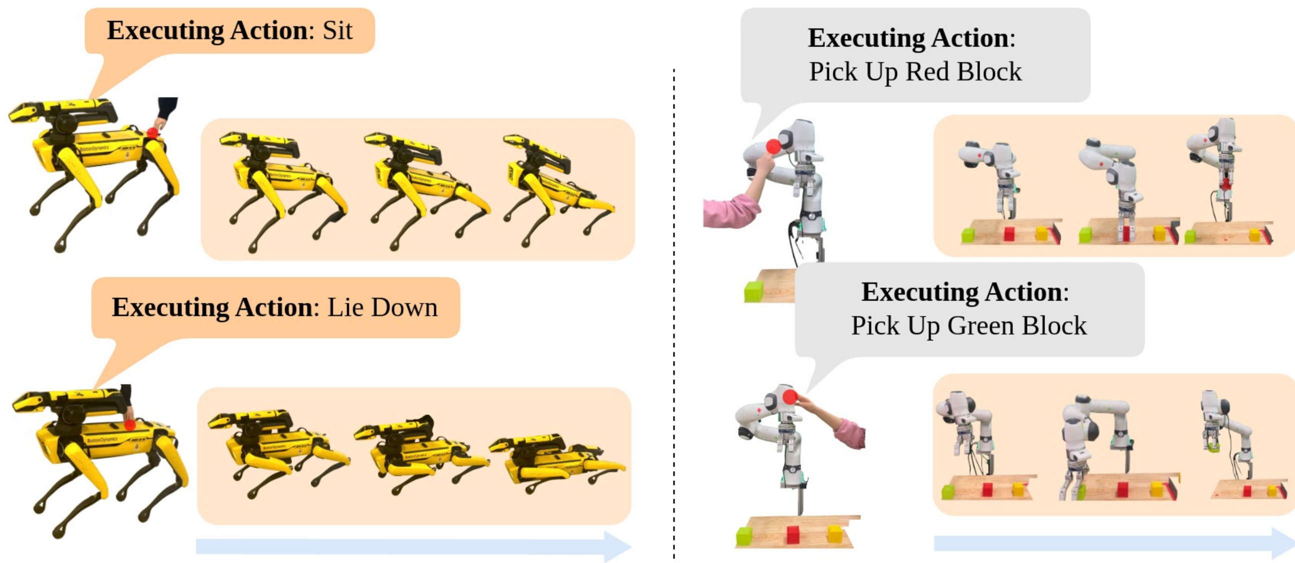

Fig. 1: **Interactions achieved using UniTac**. UniTac achieves whole-robot touch sensing without using any tactile sensors and empowers applications such as patting the quadruped for canine-inspired emotional support or touch-based instructions for manipulation. Our method can be applied to robots with different embodiment types, including quadrupeds and arms, and generalizes to different robot instances with the same type, providing a versatile interface for human-robot interactions.

***Abstract*— Robots can better interact with humans and unstructured environments through touch sensing. However, most commercial robots are not equipped with tactile skins, making it challenging to achieve even basic touch-sensing functions, such as contact localization. We present UniTac, a data-driven whole-body touch-sensing approach that uses only proprioceptive joint sensors and does not require the installation of additional sensors. Our approach enables a robot equipped solely with joint sensors to localize contacts. Our goal is to offer an off-the-shelf interface to enable robots to predict human intentions based on touch sensing capabilities, thereby providing applications such as emotional support. We validate our approach on two platforms: Franka robot arm and Spot quadruped. On Franka, we can localize contact to within 8.0 centimeters, and on Spot, we can localize to within 7.2 centimeters at around 2,000 Hz on an RTX 3090 GPU without adding any additional sensors to the robot. Our code and model will be released upon paper acceptance.**

I. Introduction

Commercial robots are becoming increasingly capable. We now have bipedal/quadrupedal robots that can walk or run in challenging environments [1–3], and robot arms that assemble products with precision [4]. Despite their impressive capabilities, they lack a critical aspect of animal behavior: physical interaction and expression of emotions through touch (Fig. 1). Consider how a simple pat can convey trust or instruction when interacting with a person or animal [5], and how a dog can express its joy by playing bow. This limitation is largely due to the absence or difficulty in endowing robots with touch-sensing capabilities. Although hardware and software advances for touch sensing have been made, the practical challenges of integrating tactile sensors into robots has prevented widespread use [6, 7].

Touch sensing is essential for a variety of physical Human-Robot Interactions (pHRI) [8], including provision of emotional support for the elderly [9] and aid in minimally invasive surgery [10], where robots assist and guide humans in shared environments. These interactions have been supported by installing dedicated tactile sensors, including sensors on robot hands [11–14], and full-body tactile skins, either rigid [15–18] or soft [19–26]. Despite their usefulness, installing these tactile sensors is error-prone and cumbersome. Rigid sensors tend to compromise the robot's dexterity and mechanical flexibility, while soft sensors are prone to damage and produce errors due to self-contact at joints [27]. Moreover, the integration of tactile sensors involves high costs and complex considerations such as calibration, power supply, wiring, and communication infrastructure [6, 28], where their versatility and reconfigurability are compromised. Alternative methods that enable robots to feel touch without dedicated tactile sensors would address these issues.

In this paper, we propose **UniTac**, a unified method to enable **whole-robot touch sensing capabilities across**

[*]Equal contribution.

[1]Department of Computer Science, Brown University, Providence, RI. Correspondence to Hongyu Li: `hli230@cs.brown.edu`

different robots without tactile sensors. Our approach is applicable to various robot platforms and leverages data from *only existing sensors*. Specifically, we use torque and position data from joint sensors, which are readily available on most commercial robots. Different contact patterns generate distinguishable proprioceptive feedback, which can be used to infer the location of contact. Unlike model-based approaches [29, 30], which depend on physical models and demand extensive expert tuning for each robot platform, our technique is entirely data-driven. Notably, our efficient data collection process requires as little as 2.5 hours (for Spot), yet it is sufficient for robust real-world whole-robot touch sensing.

We demonstrate potential applications of UniTac in pHRI. For instance, with live predictions from UniTac, a quadruped robot (Spot) can react to human touch in real time, while a Franka robotic arm can perform manipulation tasks based on the location of human contact (Fig. 1). Our evaluation shows that the accuracy of UniTac is enough to support many useful sensing abilities and human-robot interactions. This offers a flexible interface for more diverse applications: robots are able to better assist humans with physical tasks in shared environments, and to provide emotional support through touch-triggered behaviors in ways similar to animals. In summary, our contributions are as follows:

- We present a data-driven model, UniTac, that leverages built-in joint torque sensors to achieve live whole-body touch sensing across various robot platforms, eliminating the need for dedicated tactile sensors.
- UniTac demonstrates generalizability across multiple robot instances with the same type, allowing a wider community to use it as an off-the-shelf interface directly.
- We demonstrate potential applications in touch-based human-robot interaction, where the robot is able to "predict" human intentions through touch, potentially offering emotional support.

II. Method

Our goal is to develop a method for localizing touch on the robot's surface using only proprioceptive feedback. We first randomly sample a preset number of n points on the surface of the robot mesh and define them as the ground truth contact locations. We collect joint data during contact at each point multiple times by varying joint configurations, and construct a dataset $\mathcal{D} = \{d_1, d_2, \ldots, d_k\}$ with k samples. A detailed process for contact collection will be explained in the next section. Each data tuple is $d_i = (p_i, q_i, \tau_i)$, where $p \in \mathbb{R}^3$ is the ground truth contact location. $q \in \mathbb{R}^{DoF}$ and $\tau \in \mathbb{R}^{DoF}$ are the joint positions and torques, respectively. We build a contact localization model that maps the proprioceptive signal - joint positions and torques (q and τ) - to the contact coordinate (p), defined in the robot frame, using a neural network, namely **UniTac-Net**. Contact localization can be treated as either a classification or a regression problem [31, 32], which differ in the output head of the neural network.

A. Classification

When we treat it as a classification problem, we predict one of the pre-defined n points (as classes) with an additional "no-contact" class. The ground truth labels are obtained by mapping each ground truth contact location p into a one-hot encoding c with size of $(n+1)$. For the architecture, we use a four-layer MLP with layer sizes of 64, 128, 256, and 128, respectively, and a dropout rate of 0.3 after each layer. ReLU activations are used in the hidden layers, and the final layer uses a softmax activation to produce a probability distribution over the classes. We compute the cross-entropy loss between the ground truth class index c and the one-hot encoding for the predicted class index $\hat{c}$.

The classification method is robust against minor variations in joint signals because it maps inputs to a limited set of well-defined contact locations. However, it discretizes the contact space, which may limit precision if the contact point falls between the sampled points. The choice of the number of classes $(n+1)$ plays a crucial role here: increasing it can improve spatial resolution but may also make the model more complex and prone to overfitting.

B. Regression

Our regression approach directly predicts the continuous 3D coordinates of the contact point. The regression model shares the same overall structure as the classification model up to the final layer. However, the final output layer in this case has a size of three (x, y, z coordinates) and no activation function. A "no-contact" state is represented by the point (0, 0, 0). The model is trained using the mean squared error loss between ground truth p and predicted $\hat{p}$ as the loss. Compared to the classification model, the regression method avoids the inherent discretization error, potentially providing more precise localization. However, it may be more sensitive to noise in sensor readings, necessitating careful regularization and filtering. Our empirical results suggest that the regression model performs better than the classification model. Therefore, we resort to all the models used in the future sections as the regression model.

C. Training

We preprocess the data by normalizing the joint positions q and torques τ to the range of -1 to 1. This normalization, performed for each dimension across the entire dataset, helps standardize the input and speeds up the convergence of the training process. Both models are trained using the Adam optimizer [33] with a fixed learning rate of 2.5×10^{-3}. Training is conducted over 30 epochs with a batch size of 256.

D. Live Detection

UniTac-Net could run at the speed of 2,000 Hz on an NVIDIA RTX 3090 GPU. However, such a high frequency could lead to unstable predictions. Therefore, we apply an exponential moving average (EMA) filter on model predictions with a smoothing factor of 0.1 and a sliding window length of 40. This EMA filter is used to reduce noise in the output and improve temporal consistency.

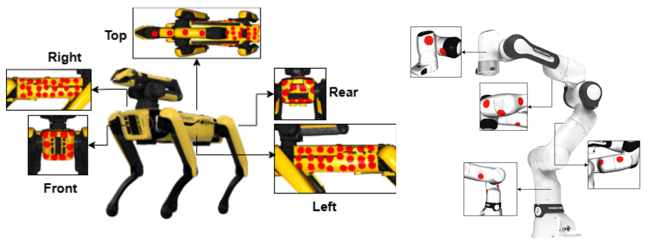

Fig. 2: **Sampled contact points for data collection.** We sample 104 points on Spot (left) and 10 points on Franka (right). Dense sampling on Spot covers the whole robot except for the legs, while the sparser sampling on Franka covers each link.

Method	Robot	Acc (%) ↑	L2 (cm) ↓
Classification	Franka	53.7	**14.8**
	Spot	54.9	**13.7**
Regression	Franka	83.5	**8.0**
	Spot	86.5	**7.2**

TABLE I: **Comparsion of model choices**. We compare the performance of our regression and classification models.

III. Experiments

We validate the effectiveness of UniTac on two platforms with distinct morphologies: the Spot quadruped from Boston Dynamics and the Franka Research 3 robotic arm from Franka Robotics. In this section, we first introduce our data collection process. Based on the collected dataset, we conduct experiments to evaluate the performance of our contact localization model. In the end, we demonstrate pHRI applications based on real-time deployment of UniTac, such as emotional support.

A. Data Collection

1) Spot: Spot (with robot arm) has a total of 19 degrees of freedom (DoF): 12 joints for the legs (3 per leg), 6 for the arm, and 1 for the gripper. In our experiments, we focused on detecting where contact occurs on the robot's body and arm while ignoring the legs for safety reasons. We sampled 104 contact points on the robot, as shown in Fig. 2 (left). The robot is kept stationary for each sample. To capture different configurations, we intentionally randomize the joint positions by teleoperating the robot into various postures (including different standing heights). Joint states for Spot are recorded using the Boston Dynamics Clients API at 60Hz.

2) Franka: FR3 model has 7 DoF. Unlike the quadruped Spot, the FR3 is more challenging for contact localization because it has an open kinematic chain with a fixed base. The robot arm joints are arranged sequentially, as opposed to the quadruped. We sample 10 points on the surface of FR3, as shown in Fig. 2 (right). The arm is assumed to be equipped with a fixed end-effector that remains steady throughout the experiments.

Data is first collected when no contact is made with the robot, in which case the robot remains stationary. Meanwhile, the visualizer window shows the robot mesh to prepare the user for the following steps. The user will then collect each selected contact location, where the visualizer shows the robot mesh with a red marker on the ground truth touch location. For data augmentation purposes, when collecting each sample, the user may vary the direction and magnitude of the touch force they apply as long as the touch location is kept the same. Spot data consists of joint state data during which contact is applied at 104 different touch locations throughout its whole body, collected over 50 sets of different joint configurations for 19 joints. In addition, data collected for FR3 consists of joint torque and joint position data during which contact is applied at 10 different touch locations across all arm links, collected over 25 sets of different joint configurations for 7 joints. These take only 2.5 hours of data collection on Spot and 12 minutes on Franka.

B. Contact Localization

1) Quantitative Results: We use two metrics to evaluate the performance of our model: L2 norm and accuracy. L2 norm is defined as the Euclidean distance $||p - \hat{p}||_2$ between the predicted position $\hat{p}$ and ground truth contact position p. Accuracy (Acc) is calculated as the percentage of predictions whose Euclidean distance from the ground truth is within a threshold ϵ. We compare our regression model with the classification model (Tab. I). When calculating the L2 norm for the classification model, the one-hot encodings are mapped back to the ground truth 3D coordinates of the contact positions. We partition the dataset into 80% for training and 20% for validation.

On Spot, the regression model achieves 86.5% accuracy (at a threshold of $\epsilon = 12$), with an average L2 error of 7.2 cm, compared to 54.9% accuracy and a 13.7 cm L2 error for the classification model. Similarly, on FR3, the regression approach attains 83.5% accuracy with an 8.0 cm L2 error, while the classification method reaches only 53.7% accuracy with a 14.8 cm L2 error. These results demonstrate that the regression model outperforms the classification model by approximately 30 percentage points in accuracy and achieves a reduction of around 6.5 cm in L2 error. This suggests that avoiding discretization leads to more precise contact localization, especially in scenarios with noisy sensor readings.

2) Qualitative Results: We demonstrate qualitative results of real-time contact localization on Spot in the video. On the Spot, we slide our touch horizontally along the left side of the body and visualize the live contact localization prediction results. The results demonstrate that our model could accurately localize rapidly changing contacts in real time. In the video, we also show that our real-time contact localization generalizes to different instances of the same robot model without additional retraining. We slide our touch horizontally along the left side of an unseen Spot robot. The contact localization results exhibit similar accuracies to the results on a seen robot.

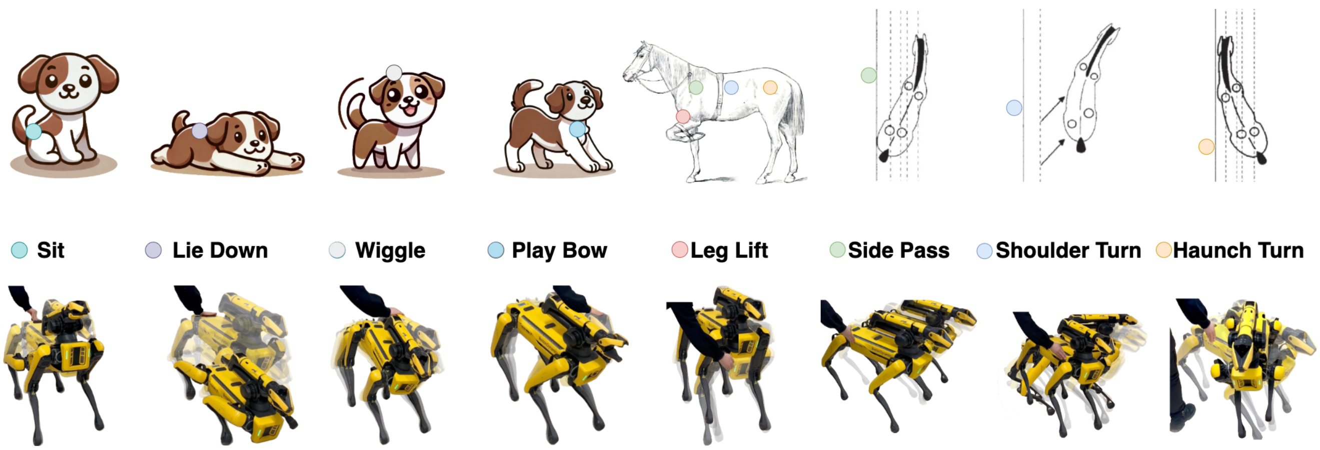

Fig. 3: **pHRI deployment on Spot.** The first row illustrates the inspiration from human-animal interactions, showcasing how dogs and horses respond to touch cues (colored dots). The second row depicts the corresponding robotic responses deployed on Spot, mimicking how animals express themselves. Video illustrations can be found in our supplementary material.

IV. pHRI Applications

In the above sections, we presented how UniTac offers a pipeline to equip a quadruped or robot arm with whole-robot touch sensing capabilities. Such tactile sensing capability equips robots with the ability to "predict" human's intentions through physical touch. In this section, we further demonstrate potential applications enabled by such whole-robot touch-sensing abilities, such as emotional support.

Humans have an innate understanding of animal behavior. Mimicking natural behaviors allows for more fluid interactions in scenarios like guiding, assisting, or responding to human intentions [34]. To illustrate how a robot can behave and interact with humans in a way similar to animals with actual touch-sensing skins, we show quadruped choreography based on localized touch. This interaction design is inspired by ethologically relevant interactions observed in human-animal communication, allowing the Spot to mimic how dogs or horses predict and react to human's expression of instructions or emotions through touch.

1) Design: We program the Spot to react to human's touch through primitive actions using its Choreography SDK. Based on the predictions from UniTac-Net, we segment the robot's body into distinct regions, each triggering a specific action (Fig. 3). We divide Spot actions into three categories: 1) Motion actions; 2) Posture change; and 3) Body expression.

Motion Actions involve whole-body movement based on horse training techniques [35] that use physical cues to guide motion. These actions respond to touch on the side faces of the robot.

- *Turning on the Forehand* is triggered by touching the upper frontal section. Spot "understands" this as instruction to turn in the opposite direction by stepping with its front legs while its hind legs step in place.
- *Turning on the Haunches* occurs when the upper dorsal section is touched. Spot "predicts" its intention as asking it to step sideways while keeping its front legs stationary.
- *Shifting on Forehand/Haunches* results from touch on the lower frontal or dorsal sections, causing a weight shift in the opposite direction, mimicking a horse's response to abdominal pressure.

Posture Change are defined as adjusting body posture from a standing position, inspired by canine social signaling. These responses are associated with touch on the top side of Spot's body.

- *Lying Down* is triggered by touching the middle section. Spot reacts by fully lowering its body.
- *Sitting* occurs when the rear section near the hip is touched, prompting Spot to lower its hindquarters, similar to a dog sitting when patted on the hip.

Body Expression represent robot actions that replicate a canine's expressive responses through movement. These behaviors are triggered by touch on Spot's arm, which corresponds to the head and upper torso of a canine.

- *Wiggling* is how Spot responds to the arm being touched.
- *Playing Bow* while opening gripper is how Spot predicts to be the intention of a human touching near the gripper – a friendly pat.

2) Spot Demonstration: Fig.3 shows how UniTac can enable promising pHRI applications for emotional support.

V. Conclusion

We present UniTac, a whole-robot touch sensing method that uses only built-in joint sensors to localize contact in real time. Our pHRI demonstrations highlight how our approach enables robots to "predict" human intentions through touch to provide emotional support. UniTac offers a robust, easy-to-deploy alternative to dedicated tactile hardware, paving the way for more reconfigurable interface for human-robot interactions. In our future work, we aim to scale up data collection to support more robust and multi-contact predictions to enrich robot reactions.

References

[1] G. Valsecchi, R. Grandia, and M. Hutter, "Quadrupedal Locomotion on Uneven Terrain With Sensorized Feet," *IEEE Robotics and Automation Letters*, vol. 5, no. 2, pp. 1548–1555, Apr. 2020, conference Name: IEEE Robotics and Automation Letters.

[2] Y. Song, S. Kim, and D. Scaramuzza, "Learning Quadruped Locomotion Using Differentiable Simulation," Oct. 2024, arXiv:2403.14864.

[3] A. Agarwal, A. Kumar, J. Malik, and D. Pathak, "Legged Locomotion in Challenging Terrains using Egocentric Vision," Nov. 2022, arXiv:2211.07638 [cs, eess].

[4] S. Haddadin, S. Parusel, L. Johannsmeier, S. Golz *et al.*, "The Franka Emika Robot: A Reference Platform for Robotics Research and Education," *IEEE Robotics & Automation Magazine*, vol. 29, no. 2, pp. 46–64, Jun. 2022, conference Name: IEEE Robotics & Automation Magazine.

[5] A. Gallace and C. Spence, "The science of interpersonal touch: an overview," *Neuroscience & Biobehavioral Reviews*, vol. 34, no. 2, pp. 246–259, 2010.

[6] R. S. Dahiya, G. Metta, M. Valle, and G. Sandini, "Tactile Sensing—From Humans to Humanoids," *IEEE Transactions on Robotics*, vol. 26, no. 1, pp. 1–20, Feb. 2010.

[7] L. Yu and D. Liu, "Recent Progress in Tactile Sensing and Machine Learning for Texture Perception in Humanoid Robotics," *Interdisciplinary Materials*, vol. n/a, no. n/a, Dec. 2024, _eprint: https://onlinelibrary.wiley.com/doi/pdf/10.1002/idm2.12233.

[8] A. De Santis, B. Siciliano, A. De Luca, and A. Bicchi, "An atlas of physical human–robot interaction," *Mechanism and Machine Theory*, vol. 43, no. 3, pp. 253–270, Mar. 2008.

[9] A. E. Block, S. Christen, R. Gassert, O. Hilliges *et al.*, "The Six Hug Commandments: Design and Evaluation of a Human-Sized Hugging Robot with Visual and Haptic Perception," in *Proceedings of the 2021 ACM/IEEE International Conference on Human-Robot Interaction*. Boulder CO USA: ACM, Mar. 2021, pp. 380–388.

[10] M. I. Tiwana, S. J. Redmond, and N. H. Lovell, "A review of tactile sensing technologies with applications in biomedical engineering," *Sensors and Actuators A: Physical*, vol. 179, pp. 17–31, Jun. 2012.

[11] H. Li, S. Dikhale, S. Iba, and N. Jamali, "ViHOPE: Visuotactile In-Hand Object 6D Pose Estimation With Shape Completion," *IEEE Robotics and Automation Letters*, vol. 8, no. 11, pp. 6963–6970, Nov. 2023.

[12] H. Li, S. Dikhale, J. Cui, S. Iba *et al.*, "HyperTaxel: Hyper-Resolution for Taxel-Based Tactile Signals Through Contrastive Learning," in *2024 IEEE/RSJ International Conference on Intelligent Robots and Systems (IROS)*, Oct. 2024, pp. 7499–7506, iSSN: 2153-0866.

[13] H. Li, M. Jia, T. Akbulut, Y. Xiang *et al.*, "V-HOP: Visuo-Haptic 6D Object Pose Tracking," Feb. 2025, arXiv:2502.17434 [cs].

[14] H. Li, J. Akl, S. Sridhar, T. Brady *et al.*, "ViTa-Zero: Zero-shot Visuotactile Object 6D Pose Estimation," Apr. 2025, arXiv:2504.13179 [cs].

[15] H. Iwate, H. Hoshino, T. Morita, and S. Sugano, "Human-humanoid physical interaction realizing force following and task fulfillment," in *Proceedings. 2000 IEEE/RSJ International Conference on Intelligent Robots and Systems (IROS 2000) (Cat. No.00CH37113)*, vol. 1, Oct. 2000, pp. 522–527 vol.1.

[16] M. Frigola, A. Casals, and J. Amat, "Human-Robot Interaction Based on a Sensitive Bumper Skin," in *2006 IEEE/RSJ International Conference on Intelligent Robots and Systems*, Oct. 2006, pp. 283–287, iSSN: 2153-0866.

[17] S.-Y. Koo, J. G. Lim, and D.-s. Kwon, *Online touch behavior recognition of hard-cover robot using temporal decision tree classifier*, Sep. 2008, journal Abbreviation: Proceedings of the 17th IEEE International Symposium on Robot and Human Interactive Communication, RO-MAN Pages: 429 Publication Title: Proceedings of the 17th IEEE International Symposium on Robot and Human Interactive Communication, RO-MAN.

[18] R. Bhirangi, V. Pattabiraman, E. Erciyes, Y. Cao *et al.*, "AnySkin: Plug-and-play Skin Sensing for Robotic Touch," Sep. 2024, arXiv:2409.08276 [cs].

[19] H. Iwata and S. Sugano, "Human-robot-contact-state identification based on tactile recognition," *IEEE Transactions on Industrial Electronics*, vol. 52, no. 6, pp. 1468–1477, Dec. 2005, conference Name: IEEE Transactions on Industrial Electronics.

[20] H. Ishiguro, T. Ono, M. Imai, T. Maeda *et al.*, "Robovie: an interactive humanoid robot," *Industrial Robot: An International Journal*, vol. 28, no. 6, pp. 498–504, Dec. 2001.

[21] T. Kanda, H. Ishiguro, T. Ono, M. Imai *et al.*, "Development and evaluation of an interactive humanoid robot "Robovie"," in *Proceedings 2002 IEEE International Conference on Robotics and Automation (Cat. No.02CH37292)*, vol. 2, May 2002, pp. 1848–1855 vol.2.

[22] T. Miyashita, T. Tajika, H. Ishiguro, K. Kogure *et al.*, "Haptic Communication Between Humans and Robots," in *Robotics Research*, S. Thrun, R. Brooks, and H. Durrant-Whyte, Eds. Berlin, Heidelberg: Springer Berlin Heidelberg, 2007, vol. 28, pp. 525–536, series Title: Springer Tracts in Advanced Robotics.

[23] N. Mitsunaga, T. Miyashita, H. Ishiguro, K. Kogure *et al.*, "Robovie-IV: A Communication Robot Interacting with People Daily in an Office," in *2006 IEEE/RSJ International Conference on Intelligent Robots and Systems*, Oct. 2006, pp. 5066–5072, iSSN: 2153-0866.

[24] T. Tajika, T. Miyashita, H. Ishiguro, and N. Hagita, "Reducing influence of robot's motion on tactile sensor based on partially linear model," in *2008 IEEE/RSJ International Conference on Intelligent Robots and Systems*, Sep. 2008, pp. 512–517, iSSN: 2153-0866.

[25] T. MINATO, M. SHIMADA, S. ITAKURA, K. LEE *et al.*, "Evaluating the human likeness of an android by comparing gaze behaviors elicited by the android and a person," *Advanced robotics : the international journal of the Robotics Society of Japan*, vol. 20, no. 10, pp. 1147–1163, 2006.

[26] H. Zhong, Y. Wang, J. Xu, Y. Cheng *et al.*, "Dynamics-Oriented Underwater Mechanoreception Interface for Simultaneous Flow and Contact Perception," *Advanced Intelligent Systems*, vol. 7, no. 1, p. 2400492, 2025.

[27] B. D. Argall and A. G. Billard, "A survey of Tactile Human–Robot Interactions," *Robotics and Autonomous Systems*, vol. 58, no. 10, pp. 1159–1176, Oct. 2010.

[28] C. Zhao, J. Ren, H. Yu, and D. Ma, "In-situ Mechanical Calibration for Vision-based Tactile Sensors," in *2023 IEEE International Conference on Robotics and Automation (ICRA)*, May 2023, pp. 10 387–10 393.

[29] M. Iskandar, A. Albu-Schäffer, and A. Dietrich, "Intrinsic sense of touch for intuitive physical human-robot interaction," *Science Robotics*, Aug. 2024, publisher: American Association for the Advancement of Science.

[30] L. Manuelli and R. Tedrake, "Localizing external contact using proprioceptive sensors: The Contact Particle Filter," in *2016 IEEE/RSJ International Conference on Intelligent Robots and Systems (IROS)*, Oct. 2016, pp. 5062–5069, iSSN: 2153-0866.

[31] A. Molchanov, O. Kroemer, Z. Su, and G. S. Sukhatme, "Contact localization on grasped objects using tactile sensing," in *2016 IEEE/RSJ International Conference on Intelligent Robots and Systems (IROS)*, Oct. 2016, pp. 216–222, iSSN: 2153-0866.

[32] J. Liang and O. Kroemer, "Contact Localization for Robot Arms in Motion without Torque Sensing," in *2021 IEEE International Conference on Robotics and Automation (ICRA)*, May 2021, pp. 6322–6328, iSSN: 2577-087X.

[33] D. P. Kingma and J. Ba, "Adam: A Method for Stochastic Optimization," Jan. 2017, arXiv:1412.6980 [cs].

[34] L. Zhan, Y. Cao, Q. Chen, H. Guo *et al.*, "Enable natural tactile interaction for robot dog based on large-format distributed flexible pressure sensors," *arXiv preprint arXiv:2303.07595*, 2023.

[35] "Chapter 6 - Communication," in *Equine Behavior*, P. McGreevy, Ed. Oxford: W.B. Saunders, Jan. 2004, pp. 151–163.